A Series of Novel Flame Retardants Produced with Nanosilica, Melamine, and Aluminum Diethylphosphinate to Improve the Flame Retardancy of Phenolic Resin

Ru Zhou, Xiaoyan Sun, Juan Xie, Gang Ma, Wen-Juan Li, Jun-Cheng Jiang, and Chi-Min Shu*

Read Online

ACCESS | Metrics & More | Article Recommendations

ABSTRACT: To facilitate the flame retardancy of phenolic resin (PF), a series of novel flame retardants with nano-SiO_2, melamine, and aluminum diethylphosphinate (ADP) were freshly prepared and tested. A thermogravimetric analysis, cone calorimeter, and scanning electron microscopy were employed to determine the thermal decomposition, flame retardancy, combustion properties, and structure of the carbon residue layer of PF. The pyrolysis kinetic parameters of modified PF were then computed, and the pyrolysis process was appraised. The results indicated that when 1.5 wt % of nano-SiO_2, 3 wt % of melamine, and 15 wt % of ADP were added to PF, the limiting oxygen index value reached 39.6%, and UL-94 passed the V-0 level. A substantial synergistic effect was also observed. The thermogravimetric analysis revealed that the char residue at 800 °C reached 59.93 wt %. Furthermore, in the cone calorimeter test, the total thermal release and thermal release rate decreased to 30.7 MJ/m^2 and 105.7 kW/ m^2, respectively.
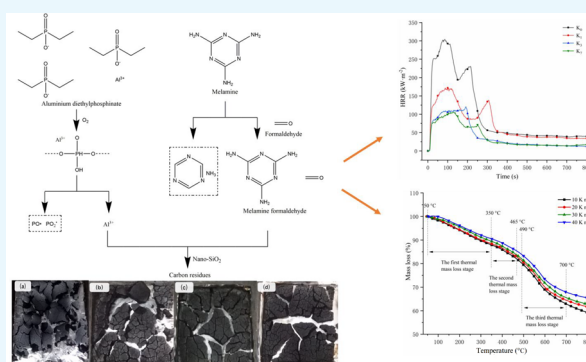
INTRODUCTION

One of the earliest polymers adapted for use in industry is phenolic resin (PF). Research on this resin has been conducted for almost a century. PF is applied as an anticorrosion and flame-retardant material and as an adhesive due to its strong acid resistance, good thermal resistance, and immaculate mechanical properties.[1] However, the mass of methine groups present in the molecule of PF means that when an external force is applied the methine bridge is readily broken, rendering it brittle and substantially limiting its applications. Apart from its structural characteristics, the secondary methyl group is effortlessly oxidized and cleaved at high temperatures. This research focuses on the enhanced fireproof and flame retardant properties of PF. This is still a hot topic in the field of polymer materials.[2]

PF is primarily modified with boron (BN), silicon, nitrogen-based, and nanoscale-phosphorus-based flame retardants. Du et al. successfully synthesized an addition-curable hybrid phenolic resin containing silicon and boron. They proved the synergistic effect of boron- and silicon-modified PF through a series of FTIR, SEM/SEM-EDS, and other experiments.[3] Chemical cross-linking generated by the two-phase interface resulted in a sealed coating of glasslike ceramics on the interface layer, which improved corrosion resistance.[4,5] Mohammed et al. found that adding boron oxide to PF could promote PF carbonization and successfully found that its

catalytic mechanism occurred in a multistage manner.[6] Li et al. employed borosilicate to modify PF. A new type of PF containing BN and silicon was prepared as part of this process. Its structure, molecular weight, curing property, gel property, and heat resistance were further characterized. Both BN and silicon were introduced to the PF to enhance thermal and oxidation resistance.[7] Xu and colleagues prepared phosphorus- and nitrogen-modified PF. Their experimental results illustrated that adding phosphorus and nitrogen to the cured resin system can produce a synergistic flame retardant effect, enhancing the flame-retardant properties of the fixed resin system and alleviating the thermal release rate. As the phosphorus and nitrogen contents increased, the flame retardant performance of the resin system increased after curing.[8]

In practice, nanomaterials are considered some of the most promising materials in the 21st century. The particle size, high surface energy, and elaborate surface coordination mean that a nano-SiO_2 amorphous white powder (referred to as its

agglomerate) can expeditiously form a bond with both itself and oxygen. This improves its intermolecular key force.[9,10] The three-dimensional mesh shape of nano-SiO_2 substantially ameliorates the material's thermal resistance.[11] It has been widely used in the modification of resin. For example, Chen et al. modified PF by coating nanosilica with graphene. A thermogravimetric (TG) experiment proved that the thermal stability of PF could be effectively improved and the carbon residue was increased by 6.54%, proving that coating nanosilica with graphene could promote the application of PF in the field of flame retardancy.[12] Noparve-Qarebagh et al. combined carbon nanotube aerogels with PF in an aerogel network to achieve a high carbon yield. Aerogel formation was confirmed using Raman spectroscopy, X-ray diffraction, and scanning electron microscopy (SEM).[13]

As one of the new flame retardants, melamine is nitrogen-based and halogen-free. The mechanical and physical properties of products can be enhanced by adding melamine. The advantages of melamine are thus clear in comparison with other flame retardants. For instance, Ge et al. modified PF by adding melamine, which indicated that 4.5 wt % was the optimal melamine composition. Moreover, the oxygen index increased and the free formaldehyde content decreased.[14]

Another new flame retardant, aluminum diethylphosphinate (ADP), has been widely applied in recent years because it is halogen-free, has excellent flame retardancy and strong thermal stability, and is outstanding in hydrophobic smoke suppression. By adding bamboo-based porous carbon and ADP to epoxy resin (EP), Wang and Hao scrutinized the action and synergistic mechanism of bamboo-based porous carbon and ADP. UL-94 vertical combustion test, limiting oxygen index (LOI), and cone calorimeter studies demonstrated that a combination of 3 wt % of the phase change material (PCM) and 4.4 wt % of ADP can increase the LOI of EP composites from 24.6 to 42.6 wt %; moreover, the UL-94 test achieved the V-0 level and the peak thermal release rate was reduced to 60.7%. Bamboo-based porous carbon and ADP have a remarkable effect on flame-retardant EP.[15]

Although research on the pyrolysis mechanics of materials has matured, it has not yet reached saturation. Kayacan and Doğan analyzed the thermal decomposition kinetics of low-density polyethylene and high-density polyethylene (HDPE). They employed TG tests to evaluate the apparent activation energy (E_a) and pre-exponential factor (A).[16] Ding et al. conducted a comparative study on the pyrolysis behavior and reaction mechanism of hardwood beech and softwood sequoia. The Flynn–Wall–Ozawa (FWO) model-free method estimated various E_a values and predicted reaction mechanisms using the Coats–Redfern model-fitting method.[17] Employing FWO, Friedman, and Kissinger–Akahira–Sunose (KAS) methods, Aboulkas et al. measured the thermal degradation behavior of polypropylene and polyethylene to obtain E_a values. They also determined the appropriate conversion of the process model using Criado and Coats–Redfern methods.[18] From these advances, this study adopted thermokinetic methods, such as FWO and KAS, to compute the E_a and A values of the chemical parameter reaction of the modified PF.[19,20]

To achieve this goal, a series of novel flame retardants with nano-SiO_2, ADP, and melamine were mixed and added to PF. Applying TGA, flame retardant tests, and cone calorimeter tests, we determined that the synergistic effect of the three flame retardants caused the modified PF to exhibit impeccable flame retardancy thermokinetics and combustion properties. In addition, Fourier-transform infrared (FTIR) spectroscopy and SEM were applied to determine the flame-retardant mechanisms of the modified PF.

◼ EXPERIMENTAL SECTION

Materials. Industrial products were chosen as the raw materials. PF was provided by Baiqian Chemical Co. (Qingdao, Shandong Province, China), and melamine (Analytical Reagent, 99%), aluminum diethylphosphinic acid (Analytical Reagent, 99.5%), and nano-SiO_2 (15 nm) were obtained from Sinopharm Chemical Reagent Co. (Nanjing, Jiangsu Province, China). Anhydrous ethanol (Analytical Reagent, 99.7%) was acquired from Yonghua Chemical Tech Co. (Shenzhen, Guangdong Province, China).

Preparation of Modified Phenolic Resin. First, a mixture of PF and anhydrous ethanol was stirred and dissolved, after which melamine, ADP, and nano-SiO_2 were added and dissolved by stirring for 1 h at 60 °C with a constant-temperature magnetic stirrer. An ultrasonic disperser was then utilized to oscillate the mixture for 30 min ultrasonically. The mixture was then left to stand for 30 min, after which the bubbles were removed. The defoamed PF hybrid solution was poured into a Teflon mold, and the mold was placed in a vacuum drying oven for temperature curing. After the spline temperature dropped to room temperature, the standard test spline of PF composite materials was removed from the mold. The three different types of flame retardants were divided into six groups by three factors and three levels through orthogonal decomposition. The factors in the orthogonal decomposition method were the reasons affecting the results. For example, ADP, melamine, and nano-SiO_2 were three factors that affected the results. Next, each element was divided into different values, called levels. The different ratios of ADP, melamine, and nano-SiO_2 are given in Table 1.

Table 1. Samples of the Modified PF with Different Additives

sample code	ADP (wt %)	melamine (wt %)	SiO_2 (wt %)
K_0	0	0	0
K_1	10.0	3.0	1.0
K_2	10.0	4.0	1.25
K_3	10.0	5.0	1.5
K_4	12.5	3.0	1.25
K_5	12.5	4.0	1.5
K_6	12.5	5.0	1.0
K_7	15.0	3.0	1.5
K_8	15.0	4.0	1.0
K_9	15.0	5.0	1.25

Testing and Characterization. The samples were characterized by infrared spectroscopy, thermogravimetry, LOI, vertical combustion, cone calorimeter, and scanning electron microscopy. First, measurements using an FTIR (Nicolet IS5 Spectrometer, Thermo Scientific, MA, USA) infrared spectrometer were recorded. Next, a SDTQ600 thermogravimetric analyzer (TA Company, DE, USA) was utilized to conduct TG experiments by heating the samples from 50 to 800 °C at a linear heating rate of 10 °C/min under a nitrogen flow of 20 mL/min. In the LOI test, 100 × 10 × 4 mm³ samples were tested using a JF-3 LOI instrument (China Jiangning Analytical Instrument Factory Co., Nanjing, Jiangsu

China) by the ISO4589-2 standard. In the UL-94 vertical combustion tests, $125 \times 13 \times 3$ mm^3 samples were tested using a CFZ-2 vertical burner (CZF-2, China Jiangning Analytical Instrument Factory). Finally, in the cone calorimeter tests (CCTs), $100 \times 100 \times 3$ mm^3 sheets were prepared and tested under a 50 kW/m^2 heat flux atmosphere using a cone calorimeter (Fire Testing Technology, West Sussex, UK) by the ISO5660 standard. Following the CCTs, the char layer of the samples was examined through SEM (a Zeiss EVO18 microscope was employed; Carl Zeiss AG, Oberkochen, Germany) to determine the morphological structure. The data of pure PF as the standard comparision sample is from our previous tests.[21]

RESULTS AND DISCUSSION

Results of Fourier Transform Infrared Analysis. Pure PF and modified PF were characterized by FTIR, as presented
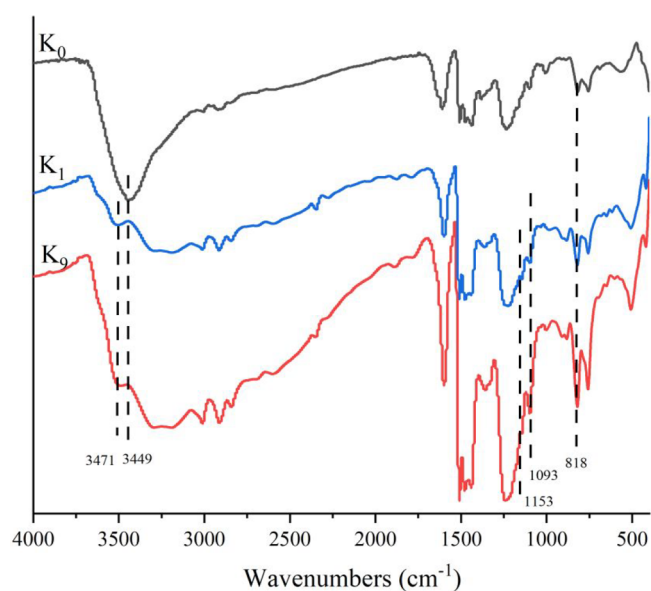
Figure 1. FTIR spectra of the PF and modified PF.
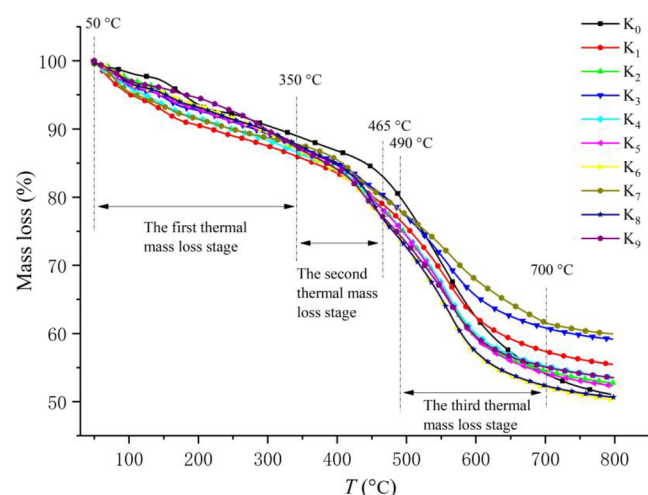
Figure 2. TG images of the modified PF samples under a nitrogen atmosphere.

in Figure 1. In comparison with the pure PF, it is concluded that the antisymmetric vibration of NH$_2$ causes the character-

Table 2. TG Data of the Pure PF and the PF Composites

sample code	$T_{5\%}$ (°C)	$T_{10\%}$ (°C)	T_{dmax} (°C)	char residue at 800 °C (wt %)
K$_0$	178.0	313.0	550.0	51.0
K$_1$	102.6	218.0	561.0	55.5
K$_2$	155.3	287.0	560.0	52.7
K$_3$	144.0	280.0	561.0	59.2
K$_4$	122.8	247.5	560.0	53.5
K$_5$	146.8	285.0	560.0	52.3
K$_6$	157.1	287.5	558.0	50.3
K$_7$	109.4	247.5	563.0	59.9
K$_8$	153.0	292.8	559.0	50.7
K$_9$	181.9	296.7	560.0	53.5

Table 3. LOI and UL-94 Results of the PF and the Modified PF

sample code	LOI (vol %)	UL-94
K$_0$	30.0	V-2
K$_1$	37.6	V-0
K$_2$	37.4	V-0
K$_3$	38.5	V-0
K$_4$	38.4	V-0
K$_5$	38.3	V-0
K$_6$	39.6	V-0
K$_7$	38.8	V-0
K$_8$	38.2	V-0
K$_9$	38.3	V-0

istic absorption peak at 3471 cm^{-1} in K$_1$ and K$_9$. At the same time, the peak at 818 cm^{-1} corresponds to the characteristic peak of the para-substituted phenol of PF. Therefore, the characteristic peak at 818 cm^{-1} can also be found in K$_0$ without melamine. However, the characteristic absorption peak at 818 cm^{-1} in the infrared images of K$_1$ and K$_9$ is caused by the deformation vibration absorption of triazine.[22] These are typical melamine characteristic peaks. A PO symmetrical stretching vibration was found at 1095 cm^{-1} and a P=C double bond appeared at 1153 cm^{-1}. These are typical ADP characteristic peaks. The 1093 cm^{-1} absorption peak was associated with a Si−O−Si antisymmetric stretching vibration, whereas the broad peak at 3449 cm^{-1} was a structural water −OH antisymmetric stretching vibration. These are typical nano-SiO$_2$ characteristic peaks. The results suggested that the ADP, melamine, and nano-SiO$_2$ were successfully incorporated into the PF matrix.

Results of Thermogravimetric Analysis. The thermal performance of both pure and modified PFs was then analyzed. Figure 2 depicts the TG curve of the samples after heating from 50 to 800 °C at a linear heating rate of 10 °C/min under a nitrogen flow of 20 mL/min. The results of $T_{5\%}$, $T_{10\%}$, and T_{dmax}, respectively representing the 5 and 10 wt % temperature and maximum mass loss rate, are summarized in Table 2. In comparison with pure PF, the $T_{5\%}$ values of PF composites with flame retardants were significantly reduced, which was believed to be due to an ethanol residue and water volatilization in PF composites. There were generally three TG stages in all of the curves, and the trend in the TG curves for the K$_1$−K$_9$ samples was similar to that for K$_0$ of the pure PF. The temperature range of the first stage is between 50 and 350 °C, and the mass loss in this stage is mainly due to the evaporation of water and the escape of excess phenols, aldehydes, and small-molecule oligomers in PF. The second

Scheme 1. Thermal Decomposition Model of Phenolic Resin Composites
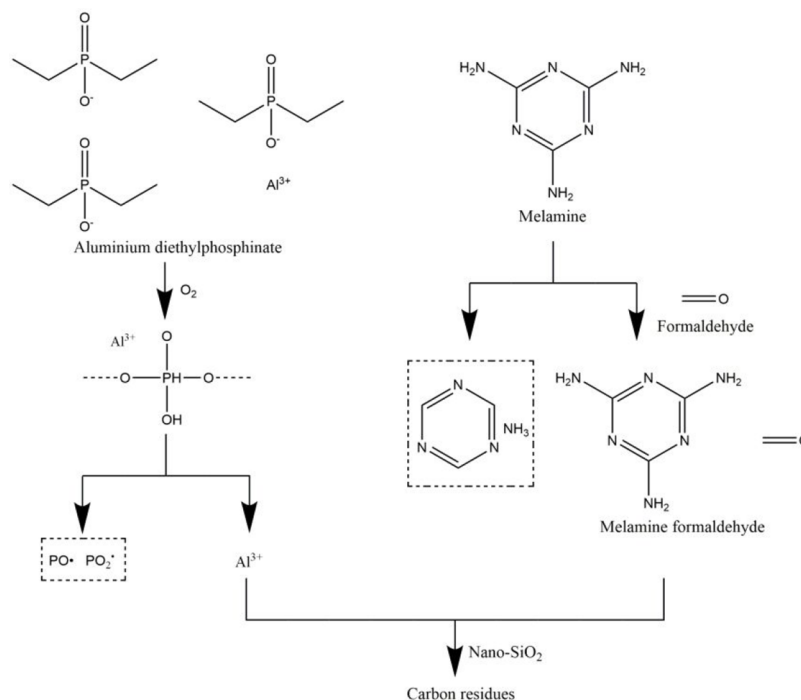
Table 4. CCT Data of the PF and the Modified PF T_{PHRR}

sample code	P_{HRR} (kW/m^2) ±30	T_{PHRR} (s) ±3	THR (MJ/m^2) ±1	P_{SPR} (m^2/s)	TTI (s) ±3	residue (wt %)
K$_0$	304.4	86.0	78.6	5.55	22	32.2
K$_1$	171.8	100.0	58.2	4.02	23	34.7
K$_3$	120.4	196.0	32.9	2.56	28	36.0
K$_7$	105.7	126.0	30.7	3.58	27	39.1

stage mainly occurs between 350 and 465 °C, mainly due to the thermal degradation of the main chain fracture of PF. The third stage is between 490 and 700 °C and is attributed to the thermal decomposition of the added flame retardants ADP, melamine, and nano-SiO$_2$. The pure PF started to decay when the temperature reached 178 °C, the thermal decomposition rate was the fastest when the temperature reached 550 °C, and the carbon residue was 51 wt % at 800 °C. As presented in Figure 2 and Table 2, the residual carbon contents of the modified PFs were 55.5%, 52.7%, 59.2%, 53.5%, 52.3%, 50.3%, 59.9%, 50.7%, and 53.5% at 800 °C, respectively. Following the addition of 1.0 wt % of nano-SiO$_2$, 3.0 wt % of melamine, and 10.0 wt % of ADP into PF, the T_{dmax} value of K$_1$ was 561 °C. The residual amount of carbon increased by 55.5% at 800 °C. In comparison with pure PF, char residues increased by 8.7%. Following the addition of 1.5 wt % of nano-SiO$_2$, 5.0 wt % of melamine, and 10.0 wt % of ADP into PF, the T_{dmax} value of K$_3$ was 561 °C, and the residual amount of carbon increased by 59.2% at 800 °C. In comparison with pure PF, char residues were augmented by 16%. Following the addition of 1.5 wt % of nano-SiO$_2$, 3.0 wt % of melamine, and 15.0 wt % of ADP to PF, the residual carbon amount increased by 17.5% in comparison with pure PF, reaching a maximum of 59.9%. This demonstrated that nano-SiO$_2$, ADP, and melamine played a synergistic role that enhanced the thermal stability of PF.

Flame-Retardant Properties of Modified Phenolic Resin. LOI and UL-94 vertical burning tests were conducted to assess flame-retardant properties of all the samples.[23] The test values are given in Table 3. As presented, the LOI of pure PF was 30.0%, but the dripping phenomenon was rarely observed in the vertical burning test due to its inherent flame retardancy. All the modified PFs were clearly at the V-0 level in the vertical burning tests. Following the addition of 12.5 wt % of ADP, 5.0 wt % of melamine, and 1.0 wt % of nano-SiO$_2$, the LOI value reached a maximum of 39.6%, higher than that of pure PF.

As observed, the optimal value of the LOI and UL-94 tests was achieved by K$_6$, which had incorporated the addition of 5.0 wt % of melamine, 12.5 wt % of ADP, and 1.0 wt % of nano-SiO$_2$, and the flame retardancy of the modified PF K$_6$ improved considerably. During the combustion process, gases from the decomposition of ADP were volatilized, and free radicals, such as PO, were generated and captured to inhibit combustion.[24,25] Furthermore, part of the residual formaldehyde was consumed in a reaction with melamine to form melamine–formaldehyde-containing nitrogen rings, which had a flame-retardant effect.[26] When the nano-SiO$_2$ added to PF was sufficient, the nanoparticles became attached to the resin molecules. Because of their strong adsorption, they were attached to the surface of the readily oxidized methylene group, thereby promoting carbonization and reducing the possibility of PF being corrupted, as showcased in Scheme 1. Moreover, the mass of Si was greater than that of C, and therefore, Si–O bonds with higher bond energy entered into the modified phenol resin. Consequently, more power generated by the PF molecular chain was absorbed, which enhanced the flame retardancy of PF.
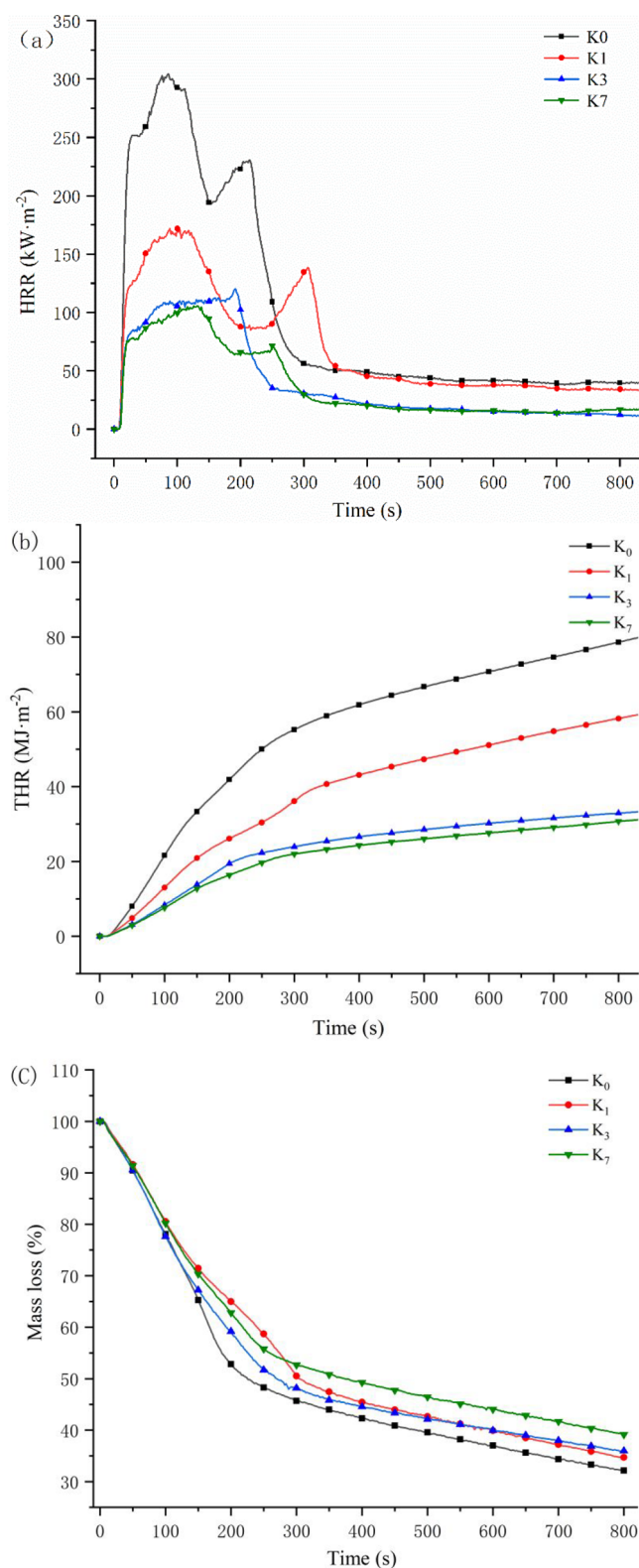
Figure 3. (a) HRR, (b) THR, and (c) mass loss of PF and modified PF.

Cone Calorimeter Test (CCT) of Modified Phenolic Resin. The CCT is one of the most effective approaches to delve into flame-retardant properties under actual fire conditions.[27] The results of the peak heat release rate (P_{HRR}), the time corresponding to P_{HRR} (T_{pHRR}), the total heat release (THR), the smoke production rate (SPR), the ignition time (TTI), and the amount of carbon residue from CCT are summarized in Table 4. The curves of HRR, THR, and the mass losses of PF and modified PF are given in Figure 3.

Following ignition, a sharp increase occurred in the HRR of pure PF. The peak value of HRR was 304.4 kW/m^2 at 86.0 s. THR reached 78.6 MJ/m^2, and the carbon residue was 32.2%. When 10.0 wt % of ADP, 3.0 wt % of melamine, and 1.0 wt % of nano-SiO$_2$ were added to PF, the HRR and THR of this K_1 group decreased to 171.8 kW/m^2 and 58.2 MJ/m^2, respectively, and the residual carbon was 34.7%.

In sharp contrast to the pure PF, the HRR and THR of K_1 decreased by 43.5% and 26.0%, respectively. Furthermore, the residual carbon increased by 7.8%. When 10.0 wt % of ADP, 5.0 wt % of melamine, and 1.5 wt % of nano-SiO$_2$ were introduced into PF, the HRR and THR of the K_3 group were reduced to 120.4 kW/m^2 and 32.9 M/m^2, respectively. According to the test data, the maximum heat release rates of K_1, K_3, and K_7 decreased and the time to reach the maximum heat release rate increased. Significantly, the time for K_3 to reach the maximum heat release rate was prolonged more obviously, which indicates that K_3 accelerates the decomposition of noncombustible gas after the temperature increases and forms a gas-phase flame-retardant environment in advance.

In even sharper contrast to the pure PF, the HRR and THR of K_3 decreased by 60.4% and 58.1%, respectively. Following the addition of 15.0 wt % of ADP, 3.0 wt % of melamine, and 1.5 wt % of nano-SiO$_2$, the HRR and THR of the K_7 group decreased to 105.7 kW/m^2 and 30.7 MJ/m^2, respectively, a decrease of 65.2% and 60.9%, which differed substantially from the values for pure PF. The residual carbon content of the K_7 group was increased by 21.4%. In contrast, the pure PF was increased by 39.1 wt %. At the same time, the P_{SPR} of pure PF decreased to 5.55 m^2/s after flame retardant was added. The modified PF K_3 was reduced by 53.9% to 2.56 m^2/s. The TTI of modified PF with flame retardant was improved in comparison with pure PF. Thus, the three flame retardants prominently decreased the HRR, THR, and PSPR of the PF and increased the residual carbon ratio of PF. Consequently, the thermal stability of PF was effectively enhanced.

Char Residue Analysis. The flame-retardant effect of the modified PF was analyzed from the residual char using a CCT. Digital photographs of the PF and selected PFs before and after the CCT are illustrated in Figures 4 and 5, respectively. According to the carbon residue content after cone combustion, the pure PF carbon residue content was 32.2 wt % at 800 °C. With the addition of flame retardants, the carbon residue content of the modified PF composite also increased. Among them, the modified PF K_1 carbon residue increased to 34.7 wt %, the modified PF K_3 carbon residue increased to 36.0 wt %, and the modified PF K_7 carbon residue was increased to 39.1 wt %. The results showed that the three flame retardants promoted the formation of PF carbon residue.[28,29]

The residual char after the CCT was analyzed using SEM, and the images are shown in Figure 6. As depicted in Figure 6a, porous holes and wide cracks are evident on the surface of the carbon layer of the pure PF. This caused the flammable, volatile gas to volatilize swiftly through the pristine PF surface during the combustion process. When ADP, melamine, and nano-SiO$_2$ were added, the carbon layer of the modified PF became more continuous, dense, and compact. However, the rigid intermolecular structure of PF was disturbed when the
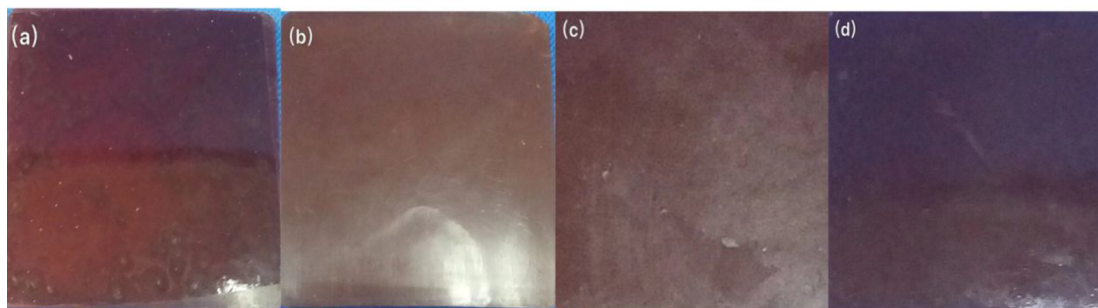
Figure 4. Digital photographs of samples taken before CCT of (a) K_0, (b) K_1, (c) K_3, and (d) K_7.
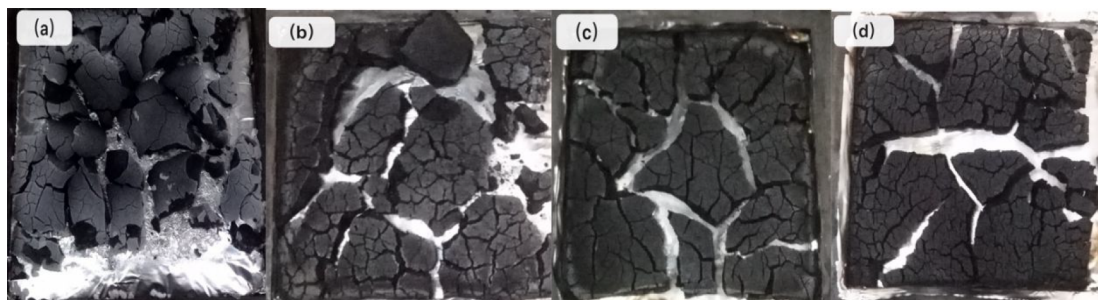
Figure 5. Digital photographs of samples taken after CCT of (a) K_0; (b) K_1, (c) K_3, and (d) K_7.
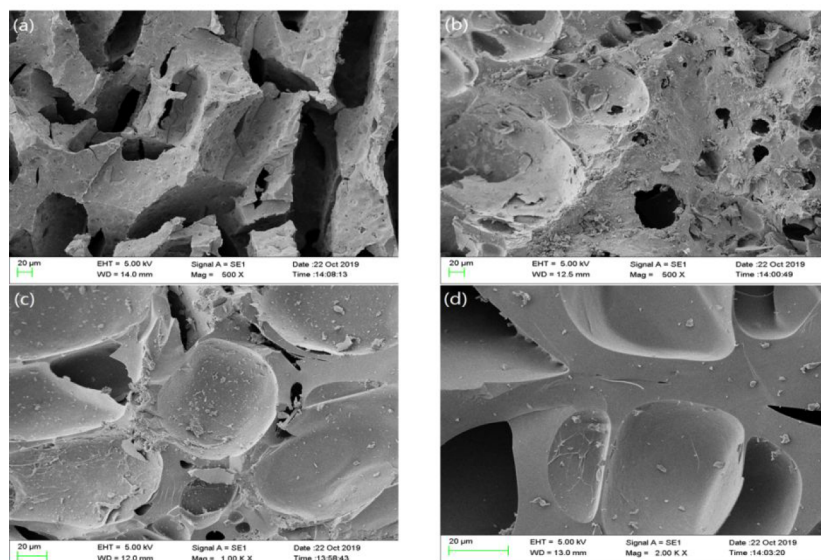
Figure 6. Electron micrographs of carbon layers after CCT of (a) K_0, (b) K_1, (c) K_3, and (d) K_7.

melamine−formaldehyde was generated, and an irregular cross-linked interpenetrating network structure was formed. Thus, the decomposition of PF was hindered.[30,31] Furthermore, the surface energy of SiO_2 was relatively low, and it migrated to the surface of the material during combustion to strengthen the carbon layer. In contrast, diethylhypophosphorous acid was formed by the degradation of ADP, and SiO_2 formed a silicon-containing phosphate to attenuate the volatilization of the phosphorus-containing compound.

Pyrolysis Kinetics Analysis of the Modified Phenolic Resin System. To conduct a thermal analysis of the materials, three factors of solution kinetics are generally required: E_a of the reaction, pre-exponential factor A, and reaction mechanism $f(\alpha)$ (mechanical function). According to the recommendations of the Kinetics Committee of the International

Confederation for Thermal Analysis and Calorimetry,[32,33] the pyrolysis process can be expressed by eq 1, illustrated as

$$\frac{d\alpha}{dt} = k(T)f(\alpha) \tag{1}$$

where α is the conversion degree during pyrolysis, $k(T)$ is the reaction rate constant and can be illuminated by Arrhenius law, and $f(\alpha)$ is a function of the reaction mechanism. Accordingly, α and $k(T)$ can be calculated from eqs 2 and 3, respectively

$$\alpha = \frac{W_0 - W_t}{W_0 - W_\infty} \tag{2}$$

$$k(T) = A \exp\left(\frac{-E_a}{RT}\right) \tag{3}$$
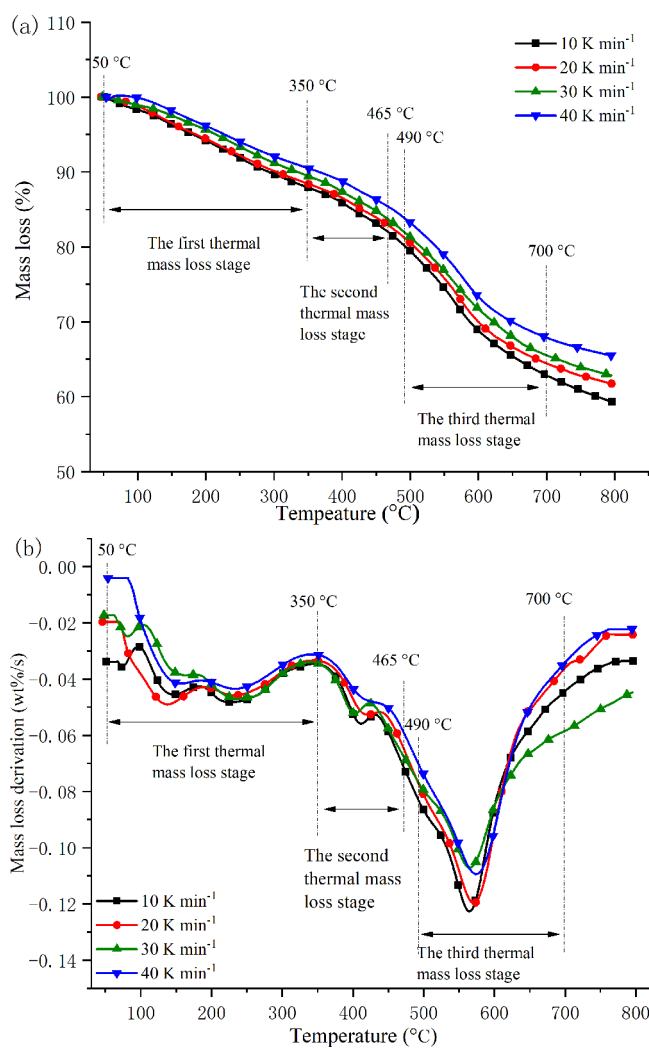
Figure 7. (a) TG and (b) DTG curves of modified PF at different heating rates.
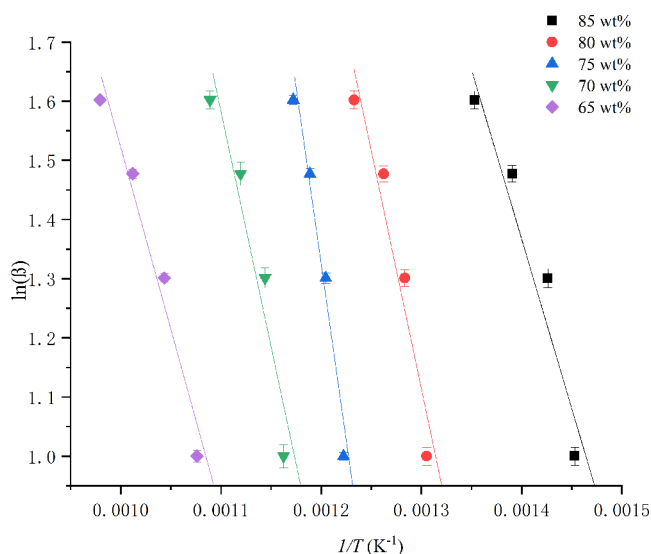
Figure 8. FWO method curves of the thermal process of modified PF from 65 to 85 wt %.

where W_0, W_t, and W_∞ represent the sample mass at the initial time, time t, and the end, respectively, A is the pre-exponential
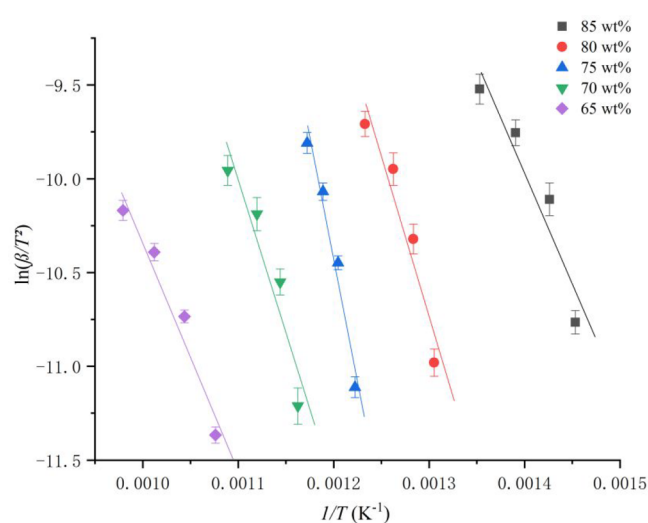
Figure 9. KAS method curves of the thermal process of modified PF from 65 to 85 wt %.

factor, E_a is the apparent activation energy of the reaction, R is the universal gas constant, and T is the reaction absolute temperature. From eqs 2 and 3, eq 4 can be expressed as follows:

$$\frac{d\alpha}{dt} = A \exp\left(\frac{-E_a}{RT}\right) f(\alpha) \tag{4}$$

Under linear heating conditions, the expression of the heating rate β is illustrated by eq 5:

$$\beta = \frac{dT}{dt} \tag{5}$$

From eqs 4, and 5, eq 6 can be expressed as follows:

$$\frac{d\alpha}{dT} = \frac{A}{\beta} \exp\left(\frac{-E_a}{RT}\right) f(\alpha) \tag{6}$$

The function of the FWO method is as follows:[34]

$$\ln \beta = \ln\left(\frac{AE_a}{RG(\alpha)}\right) - 2.315 - 0.4567\frac{E_a}{RT} \tag{7}$$

If the values of pyrolysis conversion α are the same, then $G(\alpha)$ is a constant value, and $\ln \beta$ has a linear relationship with $1/T$. The experimental pyrolysis data obtained the T value at the same conversion degree at different heating rates. Origin software was used to construct the $\ln \beta$ versus $1/T$ linear regression function graph. In conjunction with determination of the value of A, the E_a value at the conversion range was calculated directly from the slope.

The function of the KAS method is expressed as follows:[35]

$$\ln\left(\frac{\beta}{T^2}\right) = \ln\left(\frac{AR}{E_a}\right) - \frac{E_a}{RT} \tag{8}$$

Similarly to the FWO method, $\ln(\beta/T^2)$ and $1/T$ exhibit a linear relationship. The pyrolysis data obtained the T value at the same conversion degree from different heating rates. FWO and KAS methods are derived from approximate ways to solve the dynamic parameters. Therefore, there is a specific deviation between the values obtained by the two methods.

Calculation and Analysis of E_a and A. The experimental material was a sample of group K_7. Figure 7 demonstrates the

Table 5. Values of the Pyrolytic Kinetic Parameters Calculated by the FWO Method

	conversion degree (%)				
	15.0	20.0	25.0	30.0	35.0
$k = -0.4567E_a/R$	−5.772	−8.154	−11.96	−7.836	−6.145
E_a (kJ mol^{-1})	105.08	148.45	217.74	142.65	111.87
R^2	0.96081	0.90924	0.96642	0.92942	0.92738

Table 6. Values of the Pyrolytic Kinetic Parameters Calculated by the KAS Method

	conversion degree (%)				
	15.0	20.0	25.0	30.0	35.0
$k = -E_a/R$	−11.86	−17.20	−25.87	−16.27	−12.20
E_a (kJ mol^{-1})	98.61	143.01	215.10	135.28	101.44
ln A	9.11	14.46	23.86	10.67	4.38
R^2	0.94706	0.90105	0.96196	0.91661	0.90991

TG and DTG curves of the modified PF K$_7$ at heating rates of 10, 20, 30, and 40 K/min. The pyrolysis curves exhibit better consistency. As is evident from the pyrolysis curve at a heating rate of 10 K/min, the pyrolysis of modified PF K$_7$ was divided into three stages. A temperature range from 50 to 350 °C was defined as the first thermal mass loss stage. The mass loss was primarily created by the decomposition of a small number of additives due to residual moisture evaporation. The temperature range from 350 to 465 °C was defined as the second thermal mass loss stage, primarily caused by the PF primary chain fracture.[36,37] The temperature range from 490 to 700 °C was defined as the third thermal mass loss stage, which denoted secondary pyrolysis of the product of modified PF K$_7$.[38] Figure 7 indicates that the primary thermal decomposition of PF took place in the second and third stages. Therefore, the focus of this section is on presenting an analysis of the second and third stages. According to the TG/DTG curve, the main pyrolysis stage of the modified PF K$_7$ occurred from 15.0% to 35.0%. Therefore, the E_a and A of the modified PF K$_7$ in this conversion range was calculated using FWO and KAS methods.

On the basis of the five α degrees, the five corresponding fitting curves were obtained by fitting with Origin software, corresponding to five α degrees of 15.0%, 20.0%, 25.0%, 30.0%, and 35.0%. Figures 8 and 9 illustrate the fitted images for the FWO and KAS methods, respectively. Tables 5 and 6 present the E_a values calculated using the FWO and KAS methods, respectively, at different heating rates.

The fitting results indicate that the E_a calculated using both methods exhibited solid and consistent values. The E_a range of the modified PF K$_7$ composite material increased from 105.08 to 217.74 kJ/mol and from 98.61 to 215.1 kJ/mol, respectively. The E_a calculated using the FWO method was slightly larger than that derived from the KAS method, although the trend was consistent. An analysis was performed using the fitting result of the KAS method as an example, where the E_a at a conversion degree of 15.0% was 98.61 kJ/mol. As the reaction proceeded, E_a increased in line with the conversion degree and reached its maximum value of 215.1 kJ/mol when the conversion degree increased to 25.0%. Thus, the smaller the E_a, the stronger the reactivity. As the α degree increased, some substances, such as water and volatile matters, precipitated in succession, exacerbating the difficulty of continuing the reaction and raising the E_a of the material.[39] Moreover, E_a began to decrease when the pyrolysis of the modified PF K$_7$ proceeded to the α degree at 30.0%. This might have been

because the secondary pyrolysis process of the product in the third stage affected the main pyrolysis stage of the modified PF K$_7$ and therefore reduced part of E_a.

■ CONCLUSIONS

Different ratios of nano-SiO$_2$, melamine, and ADP were used and synthesized with pure PF. The FTIR results indicate that these flame retardants can be successfully added to the PF. The conclusions drawn from this study are as follows.

The relative optimized ratios of the three flame retardants were determined through TG analysis, LOI, the UL-94 test, and the CCT. Following the addition of 12.5 wt % of ADP, 5.0 wt % of melamine, and 1.0 wt % of nano-SiO$_2$, the LOI value reached a maximum of 39.6%, 32% higher than that of pure PF. According to the CCT results, with the addition of 15.0 wt % of ADP, 3.0 wt % of melamine, and 1.5 wt % of nano-SiO$_2$, the HRR, THR, and carbon residue of PF were optimal. In comparison with the values for pure PF, the HRR and THR of modified PF K$_7$ decreased by 65.2% and 60.9%, respectively.

The experimental results thus revealed that the performance of PF was optimal when 15.0 wt % of ADP, 3.0 wt % of melamine, and 1.5 wt % of nano-SiO$_2$ were added. As presented for the K$_7$ group, this was the most suitable ratio. The FWO method was employed to calculate the group's E_a range, which increased from 105.08 to 217.74 kJ/mol. In contrast, when the KAS method was used, the E_a of the modified PF K$_7$ ranged from 98.61 to 215.1 kJ/mol. The SEM results indicate that the carbon layer of the phenolic composite material became more continuous, dense, and compact. Furthermore, the large cracks and holes almost vanished due to the reaction between melamine and formaldehyde.

Nano-SiO$_2$, ADP, and melamine can exert a considerable synergistic effect in the PF, substantially enhancing its thermal stability and flame retardancy.

■ AUTHOR INFORMATION

Corresponding Author

Chi-Min Shu − Department of Safety, Health, and Environmental Engineering, School of Engineering, National Yunlin University of Science and Technology, Douliou, Yunlin 64002, Taiwan; ● orcid.org/0000-0001-9455-6162; Email: shucm@yuntech.edu.tw

Authors

Ru Zhou − Jiangsu Key Laboratory of Urban and Industrial Safety, College of Safety Science and Engineering, Nanjing

Tech University, Nanjing 211816 Jiangsu, People's Republic of China; ⊙ orcid.org/0000-0002-6851-4572

Xiaoyan Sun − *Jiangsu Key Laboratory of Urban and Industrial Safety, College of Safety Science and Engineering, Nanjing Tech University, Nanjing 211816 Jiangsu, People's Republic of China*

Juan Xie − *Jiangsu Key Laboratory of Urban and Industrial Safety, College of Safety Science and Engineering, Nanjing Tech University, Nanjing 211816 Jiangsu, People's Republic of China*

Gang Ma − *Taizhou Special Equipment Inspection and Testing Research Institute, Taizhou 318000 Zhejiang, People's Republic of China*

Wen-Juan Li − *Jiangsu Key Laboratory of Urban and Industrial Safety, College of Safety Science and Engineering, Nanjing Tech University, Nanjing 211816 Jiangsu, People's Republic of China*

Jun-Cheng Jiang − *Jiangsu Key Laboratory of Urban and Industrial Safety, College of Safety Science and Engineering, Nanjing Tech University, Nanjing 211816 Jiangsu, People's Republic of China; School of Environment & Safety Engineering, Changzhou University, Changzhou 213164 Jiangsu, People's Republic of China*

Complete contact information is available at:
https://pubs.acs.org/10.1021/acsomega.1c07246

Author Contributions

R.Z.: conceptualization, methodology, funding acquisition, and writing−review and editing. X.S.: writing−review and editing. J.X.: writing−review and editing. G.M.: software and writing− review and editing. W.-J.L.: software and writing−review and editing. J.-C.J.: supervision, project administration. C.-M.S.: project administration and writing−review and editing.

Notes

The authors declare no competing financial interest.

■ ACKNOWLEDGMENTS

■ REFERENCES

(1) Mougel, C.; Garnier, T.; Cassagnau, P.; Sintes-Zydowicz, N. Phenolic foams: A review of mechanical properties, fire resistance and new trends in phenol substitution. *Polymer* **2019**, *164*, 86−117.

(2) Liu, S.; Ning, P.; Ding, Z. Research progress in modified phenolic resin. *Therm. Resin.* **2016**, *5*, 64−70.

(3) Du, Y.; Xia, Y.; Luo, Z.; Yuan, W.; Xu, K.; Wang, Q.; Zhou, H.; Guo, Y.; Li, H.; Zhao, T. An addition-curable hybrid phenolic resin containing silicon and boron with improved thermal stability. *Polym. Degrad. Stab.* **2021**, *189*, 109599.

(4) Asaro, L.; Manfredi, L.; Pellice, S.; Procaccini, R.; Rodriguez, E. Innovative ablative fire resistant composites based on phenolic resins modified with mesoporous silica particles. *Polym. Degrad. Stab.* **2017**, *144*, 7−16.

(5) Fan, S.; Zhu, C.; Wu, D.; Wang, X.; Yu, J.; Li, F. Silicon-containing inherent flame-retardant polyamide 6 with anti-dripping via introducing ethylene glycol as the chain-linker and charring agent. *J. Polym. Degrad. Stab.* **2020**, *173*, 109080.

(6) Mohammed, M.; Alnur, S.; Aliwi, S. Study of the mechanism of graphitization of phenolic resin carbon catalyzed by boron oxide. *J. Polym. Res.* **2021**, *28*, 274.

(7) Li, Z.; Zhang, Y.; Lei, W. Phenolic resin modified by boron-silicon with high char yield. *Poly. Test.* **2019**, *73*, 208−213.

(8) Qu, L.; Sui, Y.; Zhang, C.; Dai, X.; Li, P.; Sun, G.; Xu, B.; Fang, D. Improved flame retardancy of epoxy resin composites modified with a low additive content of silica-microencapsulated phosphazene flame retardant. *React. Funct. Polym.* **2020**, *148*, 104485.

(9) Karnati, S.; Agbo, P.; Zhang, L. Applications of silica nanoparticles in glass/carbon fiber-reinforced epoxy nanocomposite. *Compos. Commun.* **2020**, *17*, 32−41.

(10) Liu, J.; Shi, B.; Su, Y.; Li, X.; Zhang, Z. Preparation of reactive nano-silica/polydimethylsiloxane composites with multiple cross-linked network structure and investigation of their mechanical properties. *Compos. Commun.* **2020**, *19*, 37−41.

(11) Wu, L.; Qi, S.; Cheng, B.; Ma, L. Research progress of PF modified by nanomaterial. *Chin. Adhes.* **2011**, *20*, 58−62.

(12) Chen, J.; Zhang, W.; Liu, J.; Ge, H.; Tian, M.; Liu, J.; Jing, M. Improved thermal stability of phenolic resin by graphene-encapsulated nano-SiO$_2$ hybrids. *J. Therm. Anal. Calorim.* **2019**, *135*, 2377−2387.

(13) Noparvar-Qarebagh, A.; Roghani-Mamaqani, H.; Salami-Kalajahi, M. Organic-inorganic nanohybrids of novolac phenolic resin and carbon nanotube: high carbon yields by using carbon nanotube aerogel and resin incorporation into aerogel network. *Mic. Mes. Mater.* **2016**, *224*, 58−67.

(14) Ge, I.; Tang, X.; Li, H. Research of phenolic resin and foam modified by melamine. *J. Shenyang U. Chem. Technol.* **2015**, *29*, 134−139.

(15) Wang, F.; Hao, J.; Li, Z.; Zou, H. Preparation of bamboo-based porous carbon material and its synergistic flame retardant epoxy resin. *Chin. J. Polym. Sci.* **2015**, *08*, 897−905.

(16) Kayacan, I.; Doğan, O. Pyrolysis of low and high density polyethylene. Part I: Non-isothermal pyrolysis kinetics. *Energy Source. Part A* **2008**, *30* (5), 385−391.

(17) Ding, Y.; Ezekoye, O. A.; Lu, S.; Wang, C.; Zhou, R. Comparative pyrolysis behaviors and reaction mechanisms of hardwood and softwood. *Energy Convers. Manage.* **2017**, *132*, 102−109.

(18) Aboulkas, A.; Harfi, K.; Bouadili, A. Thermal degradation behaviors of polyethylene and polypropylene. Part I: Pyrolysis kinetics and mechanisms. *Energy Convers. Manage.* **2010**, *51* (7), 1363−1369.

(19) Al-Salem, S.; Lettieri, P. Kinetic study of high density polyethylene (HDPE) pyrolysis. *Chem. Eng. Res. Des.* **2010**, *88* (12), 1599−1606.

(20) Xu, G.; Xu, Q.; Pan, R. R. Research on the Thermal decomposition characteristics for the thermal insulation material of EPS in air. *Plast. Ind.* **2012**, *40* (9), 67−70.

(21) Zhou, R.; Li, W.; Mu, J.; Ding, Y.; Jiang, J. Synergistic Effects of Aluminum Diethylphosphinate and Melamine on Improving the Flame Retardancy of Phenolic Resin. *Materials* **2020**, *13* (1), 158−174.

(22) Lu, C. Flame retardant and thermal degradation kinetics of PET/aluminum di-ethyl phosphinate. *Plast. Sci. Technol.* **2016**, *44*, 26−29.

(23) Wang, B.; Qian, X.; Shi, Y.; Yu, B.; Hong, N.; Song, L.; Hu, Y. Cyclodextrin microencapsulated ammonium polyphosphate: Preparation and its performance on the thermal Flame retardancy and mechanical properties of ethylene vinyl acetate copolymer. *Compos. Pt. B-Eng.* **2015**, *69*, 22−30.

(24) Pan, Y.; Song, L.; Wang, W.; Zhao, H. Polydimethylsiloxane wrapped aluminum diethylphosphinate for enhancing the flame retardancy of polyamide 6. *J. Appl. Polym. Sci.* **2020**, *137*, 49027.

(25) Ma, K.; Li, B.; Xu, M. Simultaneously improving the flame retardancy and mechanical properties for polyamide 6/aluminum diethylphosphinate composites by incorporating of 1,3,5-triglycidyl isocyanurate. *Polym. Adv. Technol.* **2018**, *29*, 1068−1077.

(26) Zhao, H.; Xie, D.; Zhang, S.; Du, F. Study on improving the high-temperature oxidation resistance of pyrolytic carbons of phenolic resin binder by in-situ formation of carbon nanotubes. *React. Funct. Polym.* **2020**, *157*, 104772.

(27) Zhou, Q.; Liu, C.; Zhou, K.; Xuan, X.; Shi, C. Synergistic effect between solid wastes and intumescent flame retardant on flammability and smoke suppression of thermoplastic polyurethane composites. *Polym. Adv. Technol.* **2020**, *31*, 4−14.

(28) Unlu, S.; Dogan, S.; Dogan, M. Comparative study of boron compounds and aluminum trihydroxide as flame retardant additives in epoxy resin. *Polym. Adv. Technol. J.* **2014**, *25*, 769−776.

(29) Wang, X.; Song, L.; Yang, H. Synergistic effect of graphene on antidripping and fire resistance of intumescent flame retardant poly(butylene succinate) composites. *Ind. Eng. Chem. Res.* **2011**, *50*, 5376−5383.

(30) Xu, S.; Qi, L.; Ma, C. Preparation and properties of modified melamine resin blended viscose fiber. *Wool. Text. J.* **2018**, *46*, 11−14.

(31) Huang, S.; Deng, C.; Zhao, Z.; Chen, H.; Gao, Y.; Wang, Y. Phosphorus-containing organic-inorganic hybrid nanoparticles for the smoke suppression and flame retardancy of thermoplastic polyurethane. *J. Polym. Degrad. Stab.* **2020**, *178*, 109179.

(32) Vyazovkin, S.; Chrissafis, K.; Lorenzo, M. ICTAC Kinetics Committee recommendations for collecting experimental thermal analysis data for kinetic computations. *Thermochim. Acta* **2014**, *590*, 1−23.

(33) Zhong, Y.; Jing, X.; Wang, S.; et al. Behavior investigation of phenolic hydroxyl groups during the pyrolysis of cured phenolic resin via molecular dynamics simulation. *Polym. Degrad. Stab.* **2016**, *125*, 97−104.

(34) Flynn, J.; Wall, L. General treatment of the thermogravimetry of polymers. *J. Res. Natl. Bur. Stand. A: Phys. and Chem.* **1966**, *70* (6), 487−493.

(35) Ceylan, S.; Topcu, Y. Pyrolysis kinetics of hazelnut husk using thermogravimetric analysis. *Bioresour. Technol.* **2014**, *156*, 182−188.

(36) Li, Q.; Xiao, Y.; Wang, C.; Deng, J.; Shu, C. Thermokinetic characteristics of coal spontaneous combustion based on thermogravimetric analysis. *Fuel.* **2019**, *250*, 235−244.

(37) Zhao, J.; Deng, J.; Wang, T.; Song, J.; Zhang, Y.; Shu, C.; et al. Assessing the effectiveness of a high-temperature-programmed experimental system for simulating the spontaneous combustion properties of bituminous coal through thermokinetic analysis of four oxidation stages. *Energy.* **2019**, *169*, 587−596.

(38) Naderi, A.; Mazinani, S.; Javad Ahmadi, S.; Sohrabian, M.; Arasteh, R. Modified thermo-physical properties of phenolic resin/carbon fiber composite with nano zirconium dioxide. *J. Therm. Anal. Calorim.* **2014**, *117* (1), 393−401.

(39) Bao, X.; Wu, F.; Wang, J. Fire retardancy and thermal degradation kinetics of epoxy composites containing polyaminoprop-yl-phenylsilsesquioxane. *J. Macromol. Sci. Part B* **2021**, *60*, 381−390.